Available online at www.sciencedirect.com
ScienceDirect
Journal of the European Ceramic Society 32 (2012) 59–70
www.elsevier.com/locate/jeurceramsoc

Effect of slurry properties and operational conditions on the structure and properties of porcelain tile granules dried in an acoustic levitator

Rosa Mondragon [a], Juan Carlos Jarque [a,*], J. Enrique Julia [b], Leonor Hernandez [b], Antonio Barba [a]

[a] *Instituto de Tecnología Cerámica, Universitat Jaume I, Campus de Riu Sec, 12071 Castellón de la Plana, Spain*
[b] *Departamento de Ingeniería Mecánica y Construcción, Universitat Jaume I, Campus de Riu Sec, 12071 Castellón de la Plana, Spain*

Received 15 April 2011; received in revised form 19 July 2011; accepted 24 July 2011

Abstract

Spray-drying is a unit operation highly important in many industrial applications. In this work, the influence of the drying conditions on the final grain properties has been investigated in single droplet experiments. Porcelain tile suspensions like those used in industry have been used. The experiments have been carried out in an acoustic levitator modified to work at high temperature conditions. The effect of the flocculation state, initial solid mass load, primary particle size, air temperature and initial droplet volume on the mean porosity of the grain and its mechanical strength has been studied. The most important parameters to be considered for the porosity are the primary particle size, the initial solid mass load and the flocculation state. For the mechanical strength the significant effects are the primary particle size, the initial solid mass load, the air temperature and the cross effect of flocculation state and initial solid mass load.

Keywords: Drying; Suspensions; Porosity; Strength; Porcelain; Acoustic levitator

1. Introduction

Porcelain tile is a very compact product, characterized by low water absorption (usually less than 0.1%).[1] It is a product with excellent technical characteristics (zero or almost zero apparent porosity, high mechanical strength and frost resistance, high hardness, and high chemical and stain resistance, etc.). The major raw materials are white-firing clays, and sodium and sodium–potassium feldspars. Other raw materials, used in minor quantities, are silica and feldspar sands, kaolins, and potassium feldspars. To enhance tile aesthetic qualities, much of the porcelain tile production is polished to provide a high-gloss surface finish, causing that certain closed pores in the tile body become visible. This apparent porosity of the polished tile, which had been closed porosity before polishing, sometimes lowers the product's stain resistance.

The industrial processing of porcelain tile includes four main stages: wet milling and homogenisation of raw materials; spray-drying of the resulting suspension to form granules; pressing of the spray-dried powder to make green compacts; and fast firing to obtain maximum densification. The slurry characteristics affect the morphology and mechanical properties of the granules which influence their compression response and therefore the structure and properties of the green and sintered bodies.

The presence of large pores in fired porcelain tile is related to the inner voids of the spray-dried powder granules. As a consequence, to produce pressed porcelain tile bodies with adequate microstructure and no defects associated with the pressing operation, high flow powders of dense and deformable granules are required. For a better understanding of the parameters affecting the granules characteristics, it is necessary to consider the development of the powder packing structure during spray drying.

Spray drying is the transformation of a given feedstock from a fluid state into a dried particulate structure by spraying the feed into a hot drying medium. Among all the industrial types of available dryers, there are few that accept pumpable fluids as feeding material at the dryer inlet and discharge dry particulates at the outlet. Among those few, spray dryers are the only ones that are able to produce powders of specific granule size and moisture content, regardless of the dryer capacity and the product heat sensitivity. These advantages have established spray dryers

* Corresponding author. Tel.: +34 964 342424; fax: +34 964 342425.
E-mail address: juancarlos.jarque@itc.uji.es (J.C. Jarque).

0955-2219/$ – see front matter © 2011 Elsevier Ltd. All rights reserved.
doi:10.1016/j.jeurceramsoc.2011.07.025

as the most important industrial fluid drying system today. In industry, spray drying is an essential unit operation for the production of powders with specific characteristics. This process is used in the manufacture of many industrial products such as ceramics, food products, detergents and pharmaceuticals.[2] The spray drying process comprises three major phases: the atomization of the liquid stream by an appropriate device to produce a spray of droplets having a high surface to volume ratio; the drying phase during which the solvent contained within the dispersion droplets is vaporized, which results in the formation of solid product particles; and the separation of the dried powder from the drying gas by an appropriate device.

The drying of a single droplet is characterized by two different drying periods.[2,3] In the first period, moisture migrates from the droplet interior rapidly enough to maintain surface saturation. As a consequence, the droplet surface is fully wetted and the mass transfer rate equals that of an equally sized pure liquid droplet. The liquid evaporates at the droplet surface and the diameter, d, decreases following the d^2-relation. This period is called the constant rate period and the maximum drying rate value is achieved. At the critical moisture content, the entire droplet surface cannot longer be maintained saturated by moisture migration and the second drying period begins. In this period, called falling rate period, a shell is formed on the droplet surface and the evaporation occurs through the pores of the shell with the vapour diffusing out to the surface. The drying rate continues to decrease as the thickness of the shell increases and the plane of evaporation moves inside the droplet. Further removal of water is a function of the moisture permeability of this shell. If the particles have been able to move or they have had enough time to diffuse inside the droplet before the shell formation, a compact grain will be formed (Fig. 1(a)). However, if the particles cannot easily move due to the suspension characteristics or the drying is so fast that there is no time for the particles to diffuse, they will remain in the outer part of the droplet and the external shell will be formed before. As a result, the grains will have a hollow morphology and a higher diameter (Fig. 1(b)).

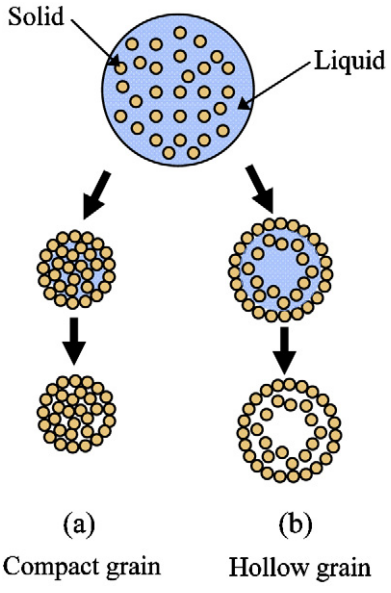

Fig. 1. Compact (a) and hollow (b) grain formation during the drying process.

Each of the above-mentioned phases, as well as their process conditions, has a huge effect on the drying process efficiency and the final product properties. In fact, despite the advantages such as rapid production, ease of automation, and no product-drying requirement, the process is prone to internal defects that can limit the quality and the strength of the final grain.[4] It is well known that the morphology, the porosity, the hollowness and the strength of the granules can vary with the process conditions. In this way, the main parameters affecting the drying process can be classified in operational conditions: inlet air temperature, relative humidity of the air, atomizing suspension feed rate and spray size distribution; and feed characteristics: initial solid mass load, primary particle size, viscosity, flocculation state and surface tension. The main objective of the researchers in this field is to know the influence of these variables on the final properties to control it and produce granules of desired characteristics suitable for each application.

The first investigations on spray drying were carried out in the 50's.[5–10] In these studies reduced scale spray dryers were used, allowing control of some of the operating variables related to the process, such as injection pressure, initial solid mass load, concentration of organic additives, temperature and humidity of the drying air, etc. The relation between the operational variables of the lab scale spray dryers and the characteristics of the final grain were investigated for pure liquids, salt solutions (ammonium nitrate, sodium sulphate, sodium silicate, sodium chloride) and food product suspensions (coffee, milk). The study of ceramic materials began in the 80's.[11–15] In these studies correlations between the slurry characteristics and the granule properties were obtained. However, the materials used (Al_2O_3, Si_3N_4, ZrO_2) were far from the compositions spray dried in the traditional ceramic industry.

The main problem with the afore-mentioned studies was that all of them were carried out in spray dryers. Inside these equipments it was not possible to fully control the parameters of the drying process. The heat and mass transfer processes were complicated to analyze due to all the interactions present in the drying system. For example heat transfer is strongly dependent upon temperature differences and, in a spray dryer, the temperature distribution in the drying gases is difficult to predict. Moreover, in a spray of wide droplet size distribution, rates of drying vary within granule size so that small sizes dries faster and have more opportunity to become overdried or overheated. Because it is not possible to obtain detailed information about isolated influence of different variables in the droplet drying process in industrial or laboratory-scaled dryers, single droplets experiments are needed.

For the study of the drying behaviour of single droplets, experiments using levitator tubes (ultrasonic, optical, electrodynamic and aerodynamic types) exhibit some advantages over conventional methods used in the first investigations to suspend individual droplets (glass filament method), since there is no mechanical contact with the droplet.[32] The experimental complexity of the ultrasonic levitators is less than the aerodynamic ones and allows working with almost any liquid over a wide

range of diameters of droplets (from 0.1 mm to several mm). However, the influence of the levitation method on the drying droplet must be considered in order to analyze the experimental results. In the case of the ultrasonic levitator, the acoustic streaming leads to a vapour enrichment around the droplet. This problem can be solved by injecting a small air flow in the chamber of the droplet, which evacuates the saturated air (ventilation). In addition, this air flow can be used to vary the temperature and humidity conditions of the drying process of the levitated droplet. The acoustic field also influences the deformation of the droplets.[16] To levitate a droplet, the ultrasound has to be strong enough to overcome gravity. However, if the sound pressure level is too high the drop disintegrates into small droplets, since the capillary forces become insufficient to keep the drop intact. Droplet evaporation results in a volume decrease: initially a levitated droplet will be deformed to an ellipsoidal shape due to the difference of radial and axial forces acting on the droplet; however as the evaporation continues the surface tension is responsible for a spherical droplet shape for small diameters.

Over the last decade, acoustic levitators have been extensively used to study the drying behaviour of pure liquids, multicomponent liquids and liquid–solid suspension droplets.[3,16–26] The use of levitators has allowed measuring the droplet shape, the evaporation rates in both drying periods, the duration of the first drying period, t_1, the final mean grain porosity, ε, and modelling the solid concentration gradient inside the droplet, predicting the appearance of hollow grains. All these studies were carried out using pure liquid droplets (water, alcohols), salt solutions and glass bead suspensions. Moreover, the drying conditions were far away from those found in industrial applications: moderate temperatures ($T < 80\,^{\circ}C$), initial droplet volumes (V_0) higher than 0.25 μl, solid mass loads (Y_S) lower than 0.3 and low relative humidity conditions ($\varphi < 4\%$). The low temperature conditions are a consequence of the ultrasonic transducer limitation, which cannot work at temperatures higher than 60 °C. Recently, Mondragon et al.,[27] have modified an ultrasonic levitator in order to work at higher temperature conditions up to 150 °C. The system has been checked in industrial operation conditions using glass bead suspensions to compare the results with previous works at low temperatures.

In this work, the drying behaviour of single droplets dried in an ultrasonic levitator and the final properties of the resulting grains were studied. All the experiments were performed using ceramic suspensions like those used in the manufacture of porcelain tiles. The rheological behaviour of the used materials was measured. The drying tests were carried out under industrial operation conditions with the modified ultrasonic levitator. The effect of the flocculation state, solid mass load (Y_S), particle size distribution of the porcelain composition (d_{P50}), ambient air temperature (T) and initial droplet volume (V_0) on the mean porosity of the grain (ε) and its mechanical strength (σ_R) was studied. Anova method was used to analyze the results and to obtain the optimal conditions of the process. The values of the input variables needed to achieve optimal output variables were discussed. For this material, the optimal conditions established according to its technical properties and manufacturing process are low porosity and good mechanical strength. The former is the most important and the lowest porosity is desirable ($\varepsilon \approx 0.24$ corresponding to the maximum packing fraction for particles with continuous size distributions), while the latter has to be high enough to resist handling and processing but not so high to easily deform during pressing process ($100\,kPa < \sigma_R < 300\,kPa$, limit values corresponding to the load resisted by a grain in a silo[33] and the apparent yield pressure at which grains start to deform, experimentally measured in an industrial powder at the standard humidity of 0.06 kg water/kg dry solid).

2. Materials, experimental set-up and measurements techniques

2.1. Materials

All the experiments were carried out with porcelain tile suspensions. The suspensions were prepared mixing water with the powder compositions elaborated from the raw materials: 45% clays, 6% sand and 49% feldspars. A standard suspension with median particle size, initial solid mass load and flocculation state similar to those found in industrial processes is established with values 3.25 μm, 0.65 (w/w) and deflocculated state, respectively.

2.2. Drying experimental set-up

The experimental set-up is composed of three systems (Fig. 2(a))[27]:

- An acoustic levitator consisting of an ultrasonic 58 kHz horn and a concave reflector (tec5 AG Sensorik und Systemtechnik). Two separated metallic chambers can be found in the

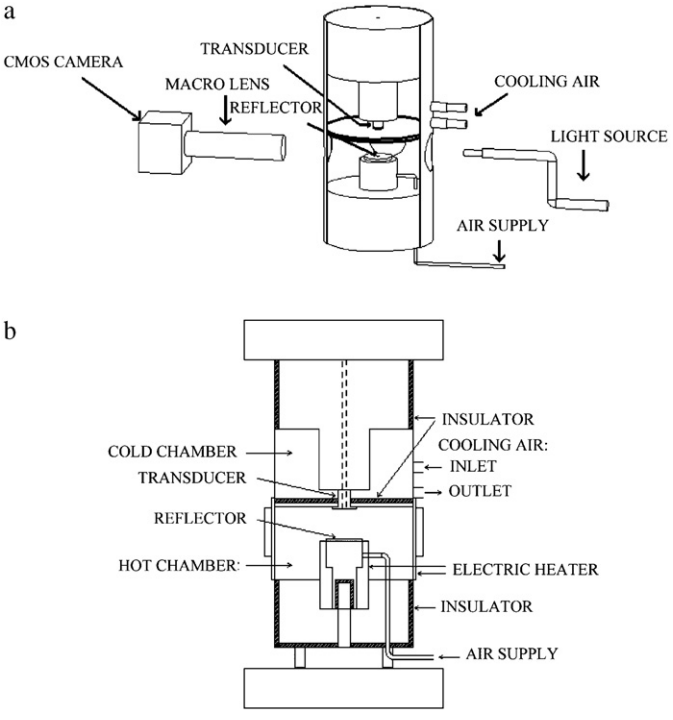

Fig. 2. General sketch of the (a) experimental set-up and (b) acoustic levitator tube.

levitator tube (Fig. 2(b)). The section identified as "cold chamber" contains the ultrasonic transducer of the levitator. The temperature is controlled by forced convection using cold air flow. The second section is identified as "hot chamber", and contains the lower part of the levitator; the reflector and the multiphase droplet. The temperature of this chamber is controlled by an electric heater at the wall and an air stream that enters the levitator tube through an array of holes located in the reflector.

- An optical system consisting of a white light source with a diffuser and a CMOS camera with a macro lens. The CMOS camera (UI-1220M, IDS-Imaging Development Systems GMBH) (752 × 480 pixels, 87 frames per second) and the back-light illumination system are used to measure the droplet cross-sectional area and the vertical position of the droplet during the drying process. The recorded images are then used to calculate the mean porosity of the grain as explained in the following sections.
- A gas conditioning system (not shown in the figure) controls the temperature, flow rate and relative humidity of the air inside the levitator tube. The air conditioning system (CEM System W-202A, Bronkhorst High-Tech B.V.) is composed of an air-drying cartridge, a two-mass flow controllers and a mixer/evaporation unit. This system allows temperatures up to 200 °C and a humidity up to a dew point of $T = 80$ °C.

2.3. Measurement techniques

The two output variables measured and analyzed in this work have been the mean grain porosity, ε, and the mechanical strength, σ_R. Each one has been obtained by means of a different technique.

The porosity has been calculated from the processing of the recorded videos. The images were processed with Matlab, so that the equivalent diameter and the position of the droplet during the drying process was obtained. Fig. 3 shows an example of the evolution of the squared equivalent diameter and position of the droplet during the drying process. Knowing the initial and final diameters of the droplet/grain and the initial properties of the droplet, the quantity of solid present inside the grain and the volume occupied can be easily obtained. With this information it is possible to know how compact the grains are and to calculate its mean porosity using the following equation[19]:

$$\varepsilon = 1 - \frac{V_S}{V_G} \tag{1}$$

where V_S and V_G are the volumes occupied by the solid phase and the dried grain, respectively and

$$V_S = V_0 Y_S \frac{\rho_D}{\rho_S} \tag{2}$$

where ρ_D and ρ_S are the densities of the liquid–solid suspension and solid phase respectively, V_0 is the initial droplet volume and Y_S is the initial solid mass load.

In order to obtain the mechanical strength of the granules, diametrical compression tests of single granules were performed. The equipment used (Instron 5889) has a special compression cell (maximum load of 10 N) that allows performing individual grain tests. Typical force–displacement curves were obtained for each experimental condition from which the fracture load of the grains was obtained. Fig. 4 shows an example of curve: it can be seen how when the compression device gets in contact with the granule, the force increases up to the breaking point. With this information, the mechanical strength of spherical bodies loaded diametrically can be calculated by means of the following equation[31]:

$$\sigma_R = 0.7 \frac{F_{max}}{\pi R^2} \tag{3}$$

where F_{max} is the maximum force resisted by the grain before breaking (as shown in Fig. 4) and R is its radius.

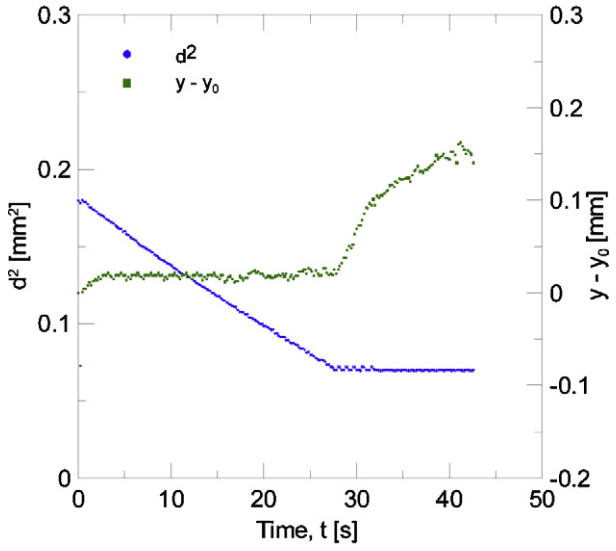

Fig. 3. Time dependence of the equivalent diameter and position of the droplet.

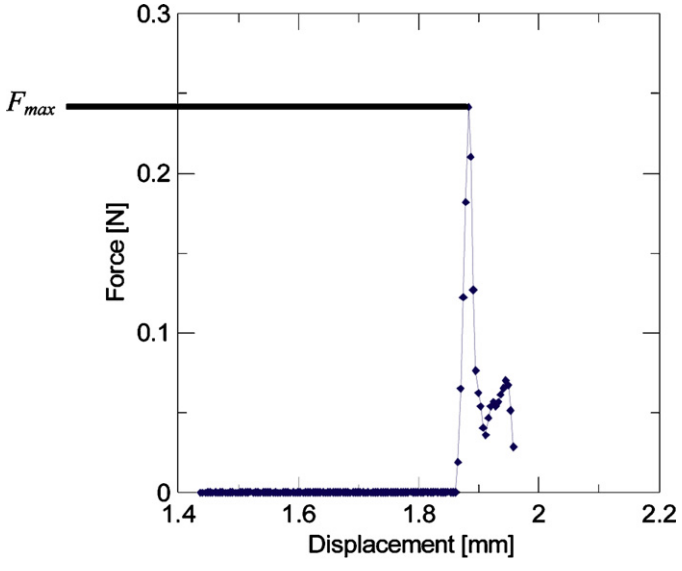

Fig. 4. Force–displacement curve for a single grain compression test.

Table 1
Input variables and their corresponding levels.

Input variables	Experimental levels
Flocculation state	Flocculated–deflocculated
Y_S	0.65–0.70 (w/w)
d_{P50}	1.95–3.25 μm
T	70–100 °C
V_0	0.4–0.7 μl

3. Experimental design and suspensions

To analyze the experimental results obtained and the influence of the input variables on the output variables, a design of experiments (DoE) was planned. In this case, a two-level factorial design was chosen to analyze the effect of five inputs. In factorial designs the effects of all the interesting factors are studied simultaneously. An important property of the full factorial designs is that all the single effects and interactions are orthogonal. It is said that the estimation of one factor is not affected by the effects of the others, simplifying the analysis of the results.

Five variables including flocculation state, initial solid mass load, Y_S, median diameter of the primary particles, d_{P50}, air temperature, T, and initial droplet volume, V_0 were chosen to study their effect on the two output variables: mean grain porosity, ε, and mechanical strength, σ_R. Table 1 summarizes the input variables and their corresponding levels.

Statgraphics was used to generate the experimental matrix, given the input levels shown in Table 1, and also to process the DoE results using analysis of variance (ANOVA). As a result, a total number of 2^5 test cases were measured. Each of the 32 conditions was repeated from four to six times in order to evaluate the reproducibility of the experimental set-up and to obtain a mean value for each output measured.

In order to reach the feed characteristics proposed in the experimental design, different compositions and suspension were studied. In next sections, the process to obtain the compositions, their particle size distribution and the rheological behaviour of the final suspensions prepared from each composition is detailed.

3.1. Compositions

The powder compositions were formulated from the corresponding raw materials. The mixture was wet ground in a laboratory ball mill where the particle size is controlled modifying the milling time. This time is adjusted so that the final particle size distribution reaches the desirable median diameter.

The industrial conditions for the particle size are those which provide a reject of 1.5–2.0% by weight on a 40 μm screen. To achieve this standard value only a 10-min milling was required. Under these conditions the obtained reject was 1.74%. Once the milling is finished, the primary particle size distribution was measured by SediGraph. The median particle size, d_{P50}, is the diameter value corresponding to a 50% of cumulative mass. The resulting median diameter for this powder composition is 3.25 μm, which is considered as standard value.

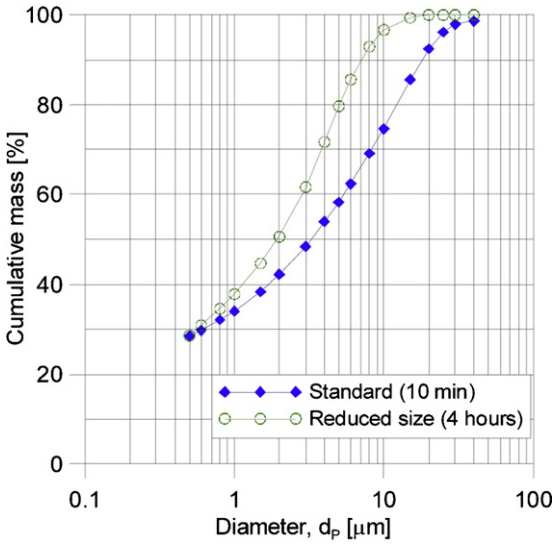

Fig. 5. Particle size distribution of the standard and the reduced size composition.

To produce a composition with a particle size distribution lower than the standard one, the milling time was increased. In this case, to obtain an appreciable reduction in the particle size, a 4-h milling was needed. Under these conditions the obtained reject was 0.04% and the median diameter of the powder was 1.95 μm. Fig. 5 shows the particle size distribution of both compositions used to prepare the ceramic suspensions: the standard composition and the reduced size composition.

3.2. Rheological behaviour

The influence of the flocculation state on the final grain properties was also studied. This variation of the suspension conditions was achieved by adding different amounts of a deflocculant additive. In this work, a $Na_5P_3O_{10}$:$Na_2O{\cdot}SiO_2$ (1:3) mixture has been used. First of all, the rheological behaviour of the suspensions and the influence of this additive on the viscosity and the thixotropy has to be known.

The viscosity of a suspension varies with the particle size and the solid mass load. In this work, the combination of the two median particle sizes (1.95 and 3.25 μm) and the two solid contents (0.65 and 0.70, w/w) results in the preparation of four different suspensions with different viscosities. For each one, the deflocculation curve has been obtained (Fig. 6). The viscosity has been measured by means of a torsion viscosimeter (Gallenkamp). In these curves it can be observed how the viscosity and the thixotropy (measured as the difference between the viscosity after 1 and 6 min) are reduced when adding the deflocculant.

To obtain slurries with different degrees of agglomeration of the particles, for each suspension previously characterized, two different amounts of additive have been chosen. In this way, the amount of deflocculant needed to achieve the deflocculated state for each case is that which provides the minimum viscosity and thixotropy. To achieve the flocculated state an amount far from the deflocculated state was chosen. In Table 2 the amounts

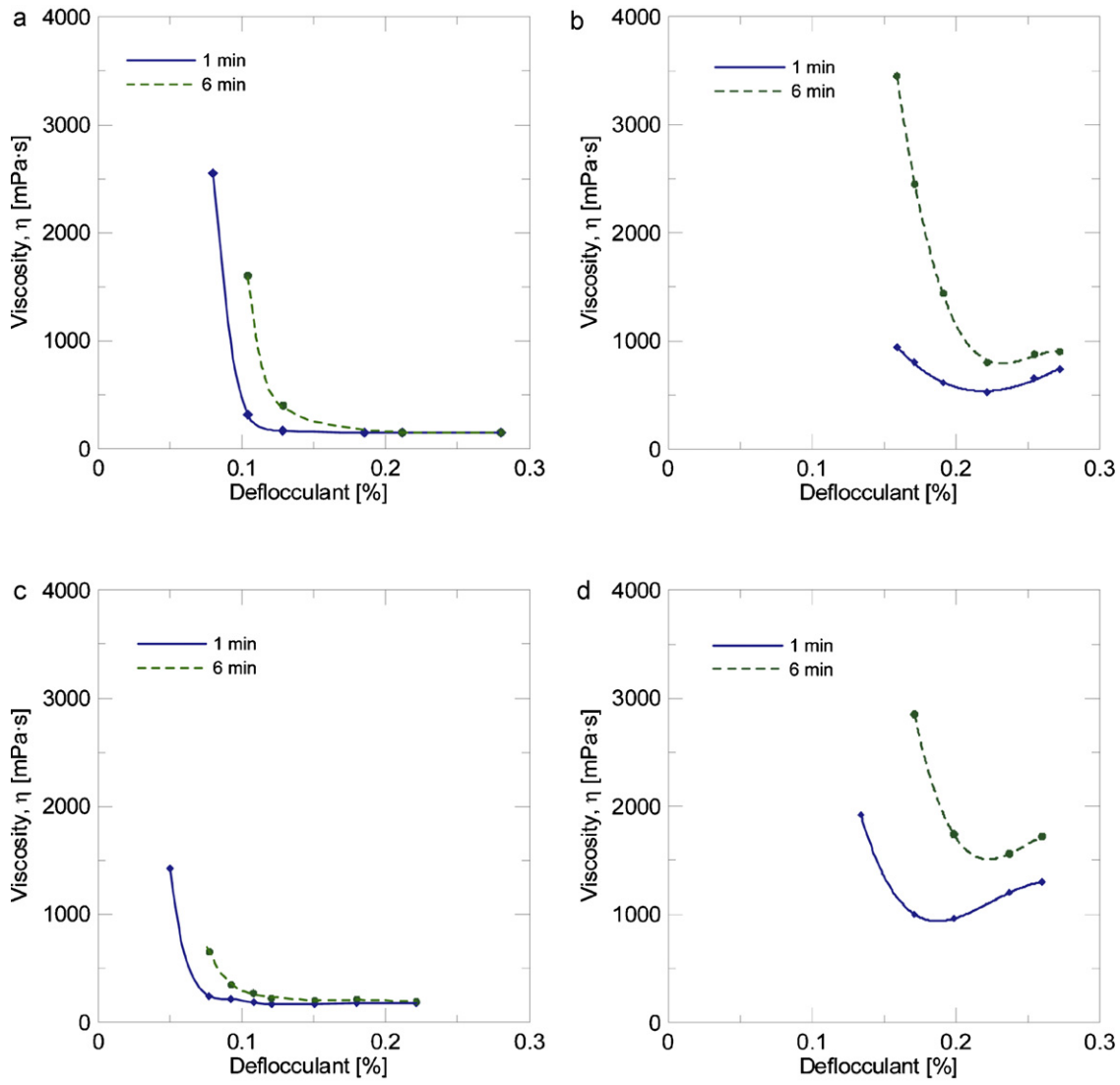

Fig. 6. Deflocculation curves: (a) $d_{P50} = 3.25$ μm, $Y_S = 0.65$ (w/w); (b) $d_{P50} = 3.25$ μm, $Y_S = 0.70$ (w/w); (c) $d_{P50} = 1.95$ μm, $Y_S = 0.65$ (w/w); (d) $d_{P50} = 1.95$ μm, $Y_S = 0.70$ (w/w).

of deflocculant additive used to prepare each suspension finally tested and the resulting viscosities are shown. The differences in viscosities and flocculation curves as a consequence of the particle size and solid content leads to different viscosities at each state for each suspension.

For each suspension (eight combinations in total) the rheogram was measured by means of a rotary viscosimeter (Fig. 7). As can be seen, the suspensions present shear-thinning behaviour in all cases. The difference of viscosities at low share rates shows the change in the flocculation state. When the shear rate is increased the flocs are broken-up, so at high shear rates, when there is no particle aggregates, both suspensions present the same viscosity.

Table 2
Amounts of deflocculant and viscosity for tested suspensions.

d_{P50} [μm]	Y_S [w/w]	Flocculation state	Deflocculant [%]	η [cP]
3.25	0.65	Flocculated	0.09	750
		Deflocculated	0.13	235
	0.70	Flocculated	0.15	1560
		Deflocculated	0.22	563
1.95	0.65	Flocculated	0.07	1840
		Deflocculated	0.13	210
	0.70	Flocculated	0.16	1720
		Deflocculated	0.19	1190

Two of the parameters most widely used to analyze the degree of flocculation are the extrapolated yield stress, τ_B, and the plastic viscosity, η_B. These parameters can be obtained adjusting the shear stress/share rate curve obtained during the viscosity test to the Bingham model:

$$\tau = \tau_B + \eta_B \cdot \gamma \quad (4)$$

where τ is the shear stress applied and γ is the shear rate generated.

Table 3 shows the values obtained for each suspension. It can be seen that the yield stress is higher for the flocculated cases than for the deflocculated ones. Due to the increase in the

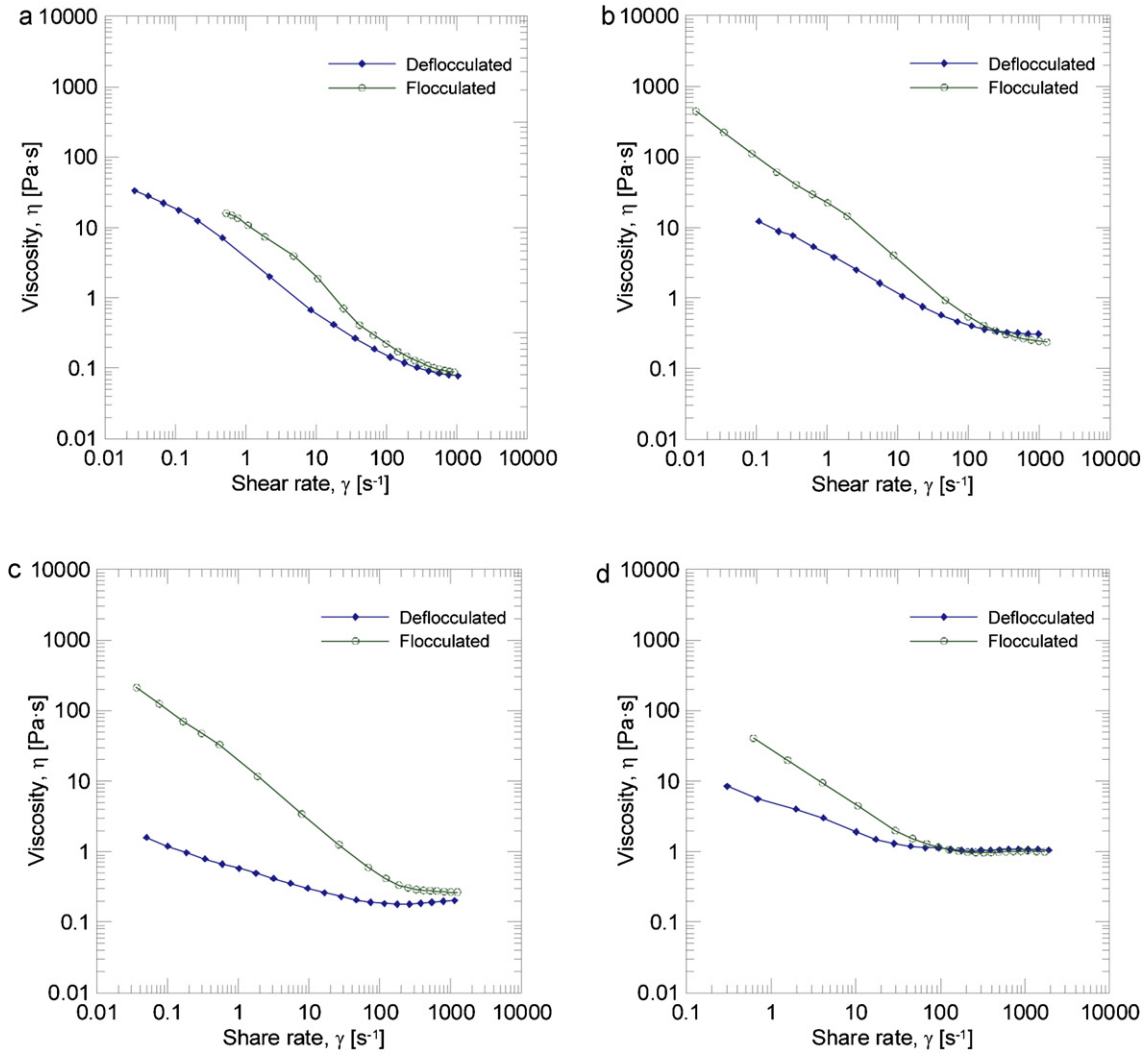

Fig. 7. Rheograms: (a) $d_{P50} = 3.25\,\mu m$, $Y_S = 0.65$ (w/w); (b) $d_{P50} = 3.25\,\mu m$, $Y_S = 0.70$ (w/w); (c) $d_{P50} = 1.95\,\mu m$, $Y_S = 0.65$ (w/w); (d) $d_{P50} = 1.95\,\mu m$, $Y_S = 0.70$ (w/w).

Table 3
Critical strain and plastic viscosity for tested suspensions.

d_{P50} [μm]	Y_S [w/w]	Flocculation state	τ_B [Pa]	η_B [Pa·s]
3.25	0.65	Flocculated	14.46	0.072
		Deflocculated	8.48	0.069
	0.70	Flocculated	32.44	0.212
		Deflocculated	10.72	0.299
1.95	0.65	Flocculated	26.33	0.193
		Deflocculated	1.21	0.178
	0.70	Flocculated	16.11	0.988
		Deflocculated	6.68	1.054

degree of agglomeration of the particles the stress required for the suspensions to flow is also increased.

4. Results and discussion

In this section the results obtained by the analysis of the experimental factorial design are discussed. Analysis of variance (ANOVA) was used to perform graphical analyses of the data and to obtain the relationship between the input variables and the responses. In the Pareto plots the most sensitive input variables can be identified. Each of these graphs shows an ordered bar chart of the standardized effects scaled by *P*-values. The vertical line corresponds with the 0.05 *P*-value which represents a significant level for achieving 95% confidence that a given effect did not just occur by chance. Positive and negative bars in the plots indicate an increasing or decreasing effect respectively of the input in the corresponding output.

Within these plots the following coding for the input variables are used: A for the flocculation state, B for the initial solid mass load (Y_S), C for the median diameter of the primary particles (d_{P50}), D for the ambient air temperature (T), and E for the initial droplet volume (V_0).

4.1. Analysis for porosity

The final mean porosity of the granules is influenced by the degree to which particles are able to rearrange and diffuse inside the droplet during the drying process and the quantity of solid

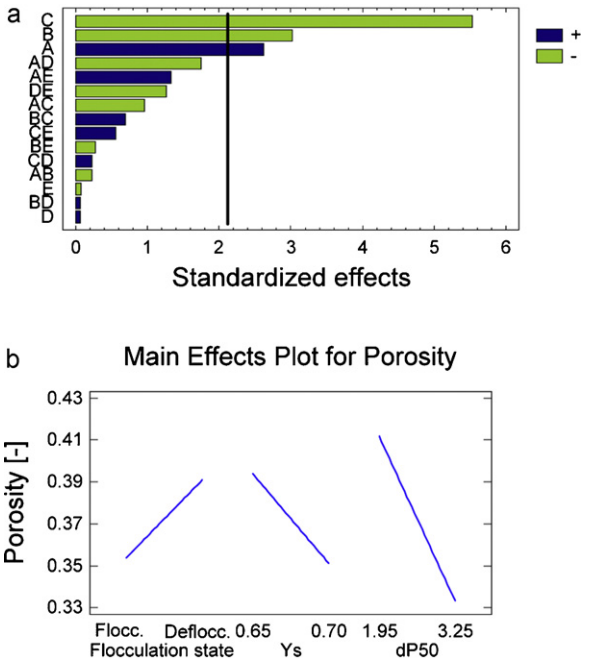

Fig. 8. (a) Standardized effects and (b) main effects for porosity.

material present. That is why in order to discuss the influence of each significant variable on the mean porosity and the degree of hollowness it is necessary to understand the process by which the grains are formed.

Fig. 8(a) shows the Pareto chart for porosity. It can be seen that the three variables which have significant effects on the porosity are the median diameter of the primary particles (C), the initial solid mass load (B) and the flocculation state (A). On the contrary, the influence of ambient air temperature and initial droplet volume on the porosity is not relevant. The significant variables for porosity are analyzed in Fig. 8(b), which shows the variation of the porosity when main effects change from lower to upper values.

It can be seen that the most important parameter that influences the porosity is the primary particle size. This input variable has a negative effect, so an increase in the size of the primary particles leads to a decrease in the mean porosity of the grains. The flow ability of suspensions is affected by the size of primary particles. Big particles have better flow ability and diffuse faster through the centre of the droplet than the small ones, so the slurry with bigger particles forms more compact structures.[28] To confirm this statement the two compositions studied have been submitted to sedimentation tests using a Turbiscan LabExpert. In these tests, the evolution of the light backscattered by the suspension due to its concentration, along the sample and over a period of 5 h, has been obtained. When the particles settle, the backscattering in the upper part decreases with time. For the composition with bigger particle size the variation rate of backscattering is 4.56%/h and after 5 h a decrease of 40.59% related to its initial value is achieved, while for the composition with smaller particle size the variation rate of backscattering is 2.29%/h and after 5 h a decrease of 20.54% is achieved. That means that bigger particles move faster than the smaller ones. Moreover, it is observed from the particle size distribution (Fig. 5) that the composition with higher median particle size (standard composition) has also a wider size distribution, defined by the ratio between d_{P90} and d_{P10}. It means that there are more particles with different sizes and thus, the small ones can fill the voids created between the big ones when these latter approach and contact them during the drying process. Therefore, an increase in the median particle size leads to a better particle-packing and a decrease in final mean grain porosity.[29]

The second important input variable affecting the mean porosity is the initial solid mass load. Its effect is also negative, so an increase in the initial mass load leads to a decrease in the mean porosity. Duffie and Marshall[8] demonstrated that the variation of the grain density between two different conditions depends on the relationship between mass load ratio and grain diameter ratio for the two conditions. When the former is bigger than the latter, it means that for a similar final grain diameter the solid material inside the grain is higher and the granules are denser. It is obvious that in droplets with equal initial volume, the higher the mass load, the higher the number of particles inside the droplet when the shell is formed.[4,30] As a result, the arrangement of the particles when the droplet dries is more uniform and the packing leads to a lower mean porosity.

Finally, the flocculation state has a positive effect. It is observed that the deflocculation of the suspension involves an increase in the mean grain porosity which leads to a hollow morphology. The formation of hollow or solid grains depends on the mobility of the particles or aggregates. In the case of flocculated suspensions, the mobility of flocs is reduced and they remain in the inner part of the droplets forming an attached structure. However, when the slurry is deflocculated, the repulsion among the particles separate them and force them to remain at the outer part of the droplet. Finally, a crater may form from the inward collapse of the surface when the particle-packing density in a droplet continues to increase after the droplet size become fixed by the formation of a rigid shell, leaving an internal void and a hollow grain.[4,13,15] As a consequence, a flocculated slurry leads to solid grains whereas a deflocculated slurry leads to hollow grains. Moreover, the deflocculant used in this work acts by a steric mechanism in which sodium silicate forms a protector colloid and sodium tripolyphosphate adsorbs over the particles leading to an increase in the effective particle volume. In this case, the repulsion makes the particles to remain even more separated from each other and closer to the surface.

Cross section of some grains has been observed by scanning electron microscopy (SEM). The biggest grains with $V_0 = 0.7$ μl (Fig. 9(a) and (b)) present hollow morphology while the smallest one with $V_0 = 0.4$ μl (Fig. 9(c)) present a larger shell thickness which makes the grain almost solid with a more homogeneously distributed porosity. From Fig. 9(a) and (b) can also be seen how the inner void formed is bigger when the suspension is deflocculated.

With all this information, if a low porosity condition is established as the optimum for the manufacturing process, the input variables must be the following: standard particle size distribution (wider distribution with higher primary particle size), high initial solid mass load and flocculated suspension. However, it

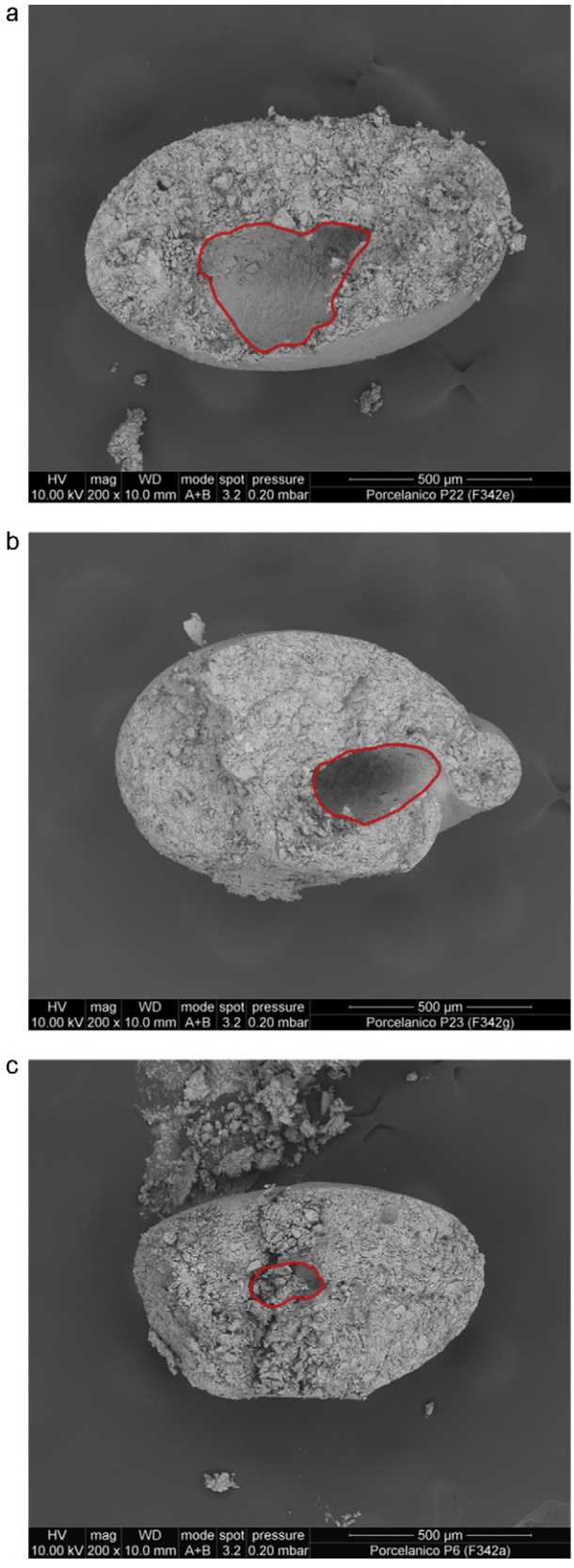

Fig. 9. Cross section of grains under different conditions: (a) $V_0 = 0.7$ μl, deflocculated, (b) $V_0 = 0.7$ μl, flocculated and (c) $V_0 = 0.4$ μl, deflocculated.

is preferred to obtain homogeneously distributed small pores than a big central one. So, although the initial droplet volume is not significant, it is desirable a small droplet volume in order to achieve a more uniformly distributed porosity, as can be concluded from SEM images. Under these conditions, the expected value for porosity obtained by means of the Anova method is 0.294 ± 0.014.

4.2. Analysis for mechanical strength

The mechanical strength of the grains is of great importance for the manufacturing process of the final product so that their quality and technical properties can be reached. This variable is related to the microstructure of the grains. In general, dense and solid granules are more resistant while the hollow ones break more easily when an external load is applied.

Fig. 10(a) shows the Pareto chart for the mechanical strength. It can be seen that the most significant effect that influences the mechanical strength is the median diameter of the primary particles (C). Effects which are also important are the initial solid mass load (B), the ambient air temperature (D) and the cross effect of flocculation state (A) and initial solid mass load

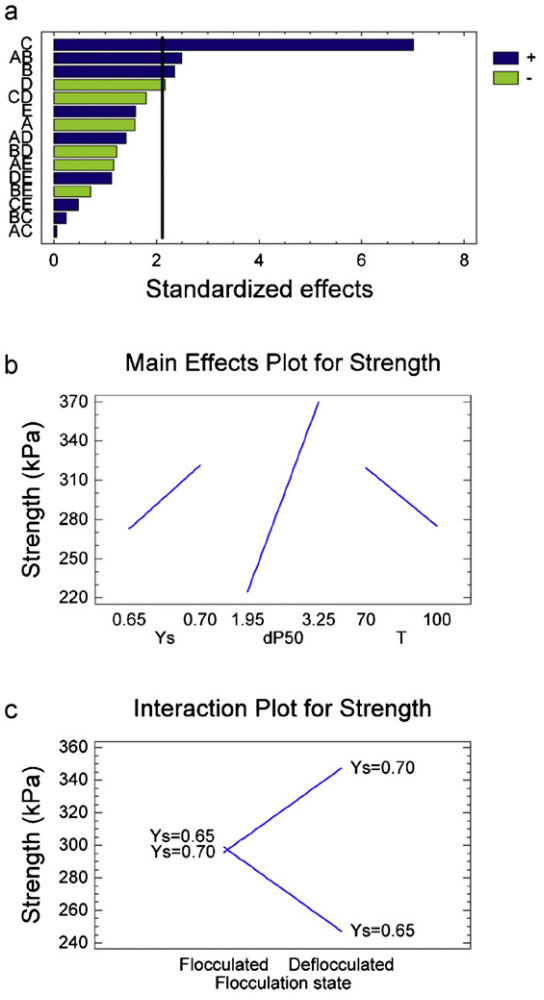

Fig. 10. (a) Standardized effects, (b) main effects and (c) cross effect for mechanical strength.

(B). In Fig. 10(b) and (c), the variation of the mechanical strength when main and cross effects change from lower to upper values, can be seen.

The effect of the input variables on the mechanical strength is inversely proportional to the effect that those variables also have on the mean porosity, i.e., the levels of the variables that produce hollow grain with higher porosity, are the same levels that lead to lower mechanical strength as expected.

The input variable that most affects the mechanical strength is the primary particle size. It has a positive effect, so an increase in the value of this input produces more resistant grains. As mentioned before, an increase in the median size of the primary particles leads to a lower porosity and more compact grains due to the better flow ability of the particles and packing. These grains are denser and their mechanical strength is higher. However, when the particle size is increased, the reactivity of the solid material during the sintering in the later firing process of the green body decreases and there are more defects in the final product related to impurities. As a consequence, a balance is needed to achieve the desirable strength.

The effect of the initial solid mass load is also positive. An increase in the solid mass load of the suspensions leads to grains with higher mechanical strength. This influence is also related to the internal morphology of the grains. When the suspension concentration is higher there are more particles in the core of the grain when the shell is formed, making them solid and denser and therefore increasing their mechanical strength.

The last main single effect is the ambient air temperature. Its effect is negative, so an increase in the air temperature leads to a decrease in the mechanical strength of the grains. When the air temperature is increased, the drying becomes faster and as a consequence, stresses inside the grains are generated. This internal microstructure favours that the grains break easier under an external force.

Finally, from the cross effect (Fig. 10(c)) it can be seen that the mechanical strength has a different behaviour depending on the values of the flocculation state and the initial solid mass load. In this way, when the suspension is flocculated, the initial solid mass load has no effect on the mechanical strength of the grains. The flocs structure formed is enough to make the grains compact and resistant independently of the quantity of particles inside the droplet. However, when the suspension is deflocculated two opposite effects appear. These effects are also related with the porosity. As mentioned before, when the suspension is deflocculated the particles remain separated from each other at the outer part of the grain, forming an external shell. Under these conditions, if the mass load is low, all the particles are in the shell and the grains are hollow with a lower mechanical strength. On the contrary, if the suspension is deflocculated but the solid mass load is higher, there are more particles inside the droplet when the shell is formed and the mechanical strength is higher.

With all this information, if a high mechanical strength condition is searched as the optimum for the manufacturing process, the input variables must be the following: standard primary particle size distribution (wider distribution with higher median particle size), high initial solid mass load, low ambient air temperature and deflocculated suspension. Under these conditions the expected value for mechanical strength obtained by means of the Anova method is 442 ± 24 kPa.

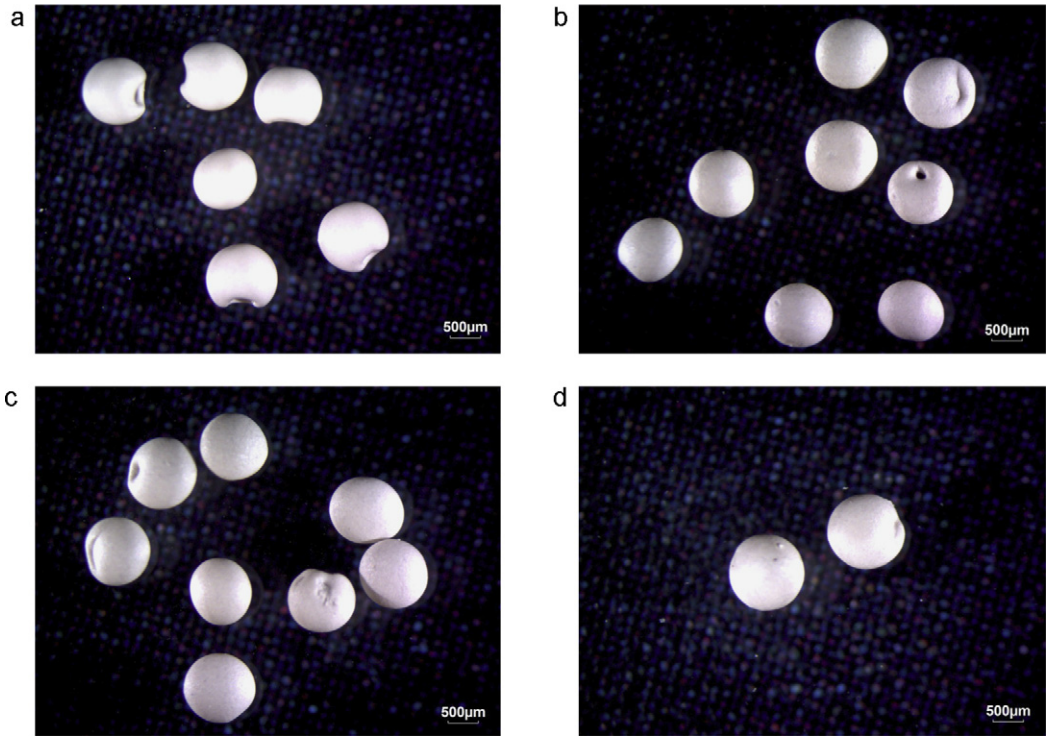

Fig. 11. Morphology of grains obtained under different experimental conditions: (a) deflocculated, $Y_S = 0.65$ (w/w), $d_{P50} = 1.95$ µm; (b) deflocculated, $Y_S = 0.65$ (w/w), $d_{P50} = 3.25$ µm; (c) flocculated, $Y_S = 0.70$ (w/w), $d_{P50} = 3.25$ µm; (d) deflocculated, $Y_S = 0.70$ (w/w), $d_{P50} = 3.25$ µm.

The two first conditions are the same that those required for a low porosity, but the deflocculation state is different. However, in this case the highest strength is not desirable. Actually, it has to be high enough to resist handling and processing but small enough to allow an easy deformation during pressing process. Considering that the maximum load that supports a grain inside a conventional storage silo is 100 kPa, the optimum value obtained is very high. Therefore, it is more important to know the conditions that provide the lowest porosity and check if the mechanical strength is appropriate for the process. In this case, the mechanical strength obtained under the optimal conditions established for the porosity is 277 kPa, which is enough for handling, etc.

4.3. Morphology

In order to know if the input variables that have significant effects on the porosity also influence the grain morphology, grains obtained under different experimental conditions have been observed by means of an optical microscope (Fig. 11).

It can be seen that there are no important differences among Fig. 11(b)–(d), where the influence of the flocculation state and the initial solid mass load on the final morphology can be observed. Fig. 11(a) is the only one which presents a different morphology. In this case, where the primary particle size is the reduced one, all the grains present a crater. The primary particle size is the variable that presents the most important effect on the two output variables of the experimental design. That means that under these conditions, the shell is formed faster than under the other conditions that also lead to a shell formation. As a consequence, in this case the quantity of water retained inside the grain is higher. When all this water is evaporated the level of pressure inside the grain is so high that a crater is form to allow the vapour to get out of the grain.

5. Conclusions

A standard levitator tube modified to work at high temperature conditions (drying temperature up to 120 °C) has been used for the first time to obtain grains similar to industrial ones, dried under the same conditions. Single droplets of ceramic suspensions with the same characteristics that those used in the manufacture of porcelain tiles have been dried. The ability of the equipment to study the drying behaviour of this kind of suspensions with high mass load and viscosity has been checked.

The flocculation state, the initial solid mass load, the primary particle size distribution of the porcelain composition, the ambient air temperature and the initial droplet volume have been modified to study their effect on the mean porosity of the grain and its mechanical strength and to establish the optimal conditions of the process. A factorial design has been used to better analyze all the results obtained by means of the ANOVA method.

In this way, the significant effects that influence porosity are the primary particle size of the composition, the initial solid mass load and the flocculation state. If low porosity grains are desirable, standard particle size distribution (wider distribution with higher median particle size), high initial solid mass load and flocculated suspension is needed. Moreover, small initial droplet volume gives a more uniformly distributed porosity.

For the mechanical strength, the significant effects are the primary particle size of the composition, the initial solid mass load, the ambient air temperature and the cross effect of flocculation state and initial solid mass load. If grains with high mechanical strength are desirable, standard particle size distribution (wider distribution with higher median particle size), high initial solid mass load, low ambient air temperature and deflocculated suspension are required.

Finally, the primary particle size is the only parameter which presents a significant influence on the final morphology of the grains. To avoid the presence of craters in the grains a distribution with high median particle size has to be used. This condition also favours the two final properties studied in this work.

Acknowledgments

The authors gratefully acknowledge the financial support from Fundació Caixa Castelló-Bancaixa (projects P11B2006-37 and P11B2009-27).

R. Mondragón thanks the Spanish Ministry of Education for a pre-doctoral fellowship (FPU program, Ref. AP2008-01077).

References

1. Brusa A, Contoli L, Dardi M. Fine porcelainized stoneware. Sacmi; 1989.
2. Masters K. Spray drying handbook. Longman Scientific and Technical; 1991.
3. Kastner O, Brenn G, Rensink D, Tropea C. Modeling and experimental investigation of the morphology of spray dried particles. *Chem Eng Technol* 2001;**24**:335–9.
4. Walker WJ, Reed JS. Influence of slurry parameters on the characteristics of spray-dried granules. *J Am Ceram Soc* 1999;**82**:1711–9.
5. Ranz WE, Marshall WR. Evaporation from drops. Part 1. *Chem Eng Prog* 1952;**48**:141–6.
6. Ranz WE, Marshall WR. Evaporation from drops. Part 2. *Chem Eng Prog* 1952;**48**:173–80.
7. Duffie JA, Marshall WR. Factors influencing the properties of spray-dried materials. Part I. *Chem Eng Prog* 1953;**49**:417–23.
8. Duffie JA, Marshall WR. Factors influencing the properties of spray-dried materials. Part II. Drying studies. *Chem Eng Prog* 1953;**49**:480–6.
9. Crosby EJ, Marshall WR. Effects of drying condition on the properties of spray-dried particles. *Chem Eng Prog* 1958;**54**:56–63.
10. Charlesworth CH, Marshall WR. Evaporation from drops containing dissolved solids. *AIChE J* 1960;**6**:9–23.
11. Lukasiewicz SJ. Spray-drying ceramic powders. *J Am Ceram Soc* 1989;**72**:617–24.
12. Takahashi H, Shinohara N, Okumiya M. Influence of slurry flocculation on the character and compaction of spray-dried silicon nitride granules. *J Am Ceram Soc* 1995;**78**:903–8.
13. Bertrand G, Filiatare C, Mahdjoub H, Foissy A, Coddet C. Influence of slurry characteristics on the morphology of spray-dried alumina powders. *J Eur Ceram Soc* 2003;**23**:263–71.
14. Bertrand G, Roy P, Filiatare C, Coddet C. Spray-dried ceramic powders: a quantitative correlation between slurry characteristics and shapes of the granules. *Chem Eng Sci* 2005;**60**:95–102.
15. Zainuddin MI, Tanaka S, Furushima R, Uematsu K. Correlation between slurry properties and structures and properties of granules. *J Eur Ceram Soc* 2010;**30**:3291–6.
16. Yarin AL, Weiss DA, Brenn G, Rensink D. Acoustically levitated drops: drop oscillation and break-up driven by ultrasound modulation. *Int J Multiphase Flow* 2002;**28**:887–910.

17. Brenn G, Kastner O, Rensink D, Tropea C. Evaporation and drying of multicomponent and multiphase droplets in a tube levitator. In: *Proc of the 15th annual conf liquid atomiz and spray syst (ILASS Europe)*. 1999.
18. Brenn G. Concentration fields in evaporating droplets. *Int J Heat Mass Transfer* 2005;**48**:395–402.
19. Kastner O, Brenn G, Rensink D, Tropea C, Yarin AL. Investigation of the drying behaviour of suspension droplets in an acoustic tube levitator. In: *Proc 16th annual conf liquid atomiz and spray syst (ILASS Europe)*. 2000.
20. Kastner O, Brenn G, Rensink D, Tropea C. Mass transfer from multiphase droplets during drying in a tube levitator. In: *Proc 8th int conf liquid atomiz and spray syst*. 2000.
21. Kastner O, Brenn G, Rensink D, Tropea C. The acoustic tube levitator: a novel device for determining the drying kinetics of single droplets. *Chem Eng Technol* 2001;**24**:335–9.
22. Kastner O, Brenn G, Tropea C. The drying time of single suspension droplets under various conditions. In: *Proc conference "spray drying and related processes"*. 2001. p. 1–8, paper 1.
23. Yarin AL, Brenn G, Kastner O, Rensink D, Tropea C. Evaporation of acoustically levitated droplets. *J Fluid Mech* 1999;**399**:151–204.
24. Yarin AL, Brenn G, Kastner O, Tropea C. Drying of acoustically levitated droplets of liquid–solid suspensions: evaporation and crust formation. *Phys Fluids* 2002;**14**:2289–98.
25. Zaitone B, Hunsmann S, Castanet G, Damaschke N, Ebert V, Tropea C. Evaporation of acoustically levitated droplets. In: *Proc 10th int congress on liquid atomiz and spray syst*. 2006.
26. Zaitone B, Frackowiak B, Tropea C. Drying of multiphase single droplets: two dimensional modelling. In: *Proc 16th int drying symposium*. 2008.
27. Mondragon R, Hernandez L, Julia JE, Jarque JC, Chiva S, Zaitone B, et al. Study of the drying behavior of high load multiphase droplets in an acoustic levitator at high temperature conditions. *Chem Eng Sci* 2011;**66**(12):2734–44.
28. Wang AJ, Lu YP, Sun RX. Recent progress on the fabrication of hollow microspheres. *Mater Sci Eng A* 2007:460–1.
29. Dias RP, Teixeira JA, Mota MG, Yelshin AI. Particulate binary mixtures: dependence of parking porosity on particle size ratio. *Ind Eng Chem Res* 2004;**43**:7912–9.
30. Sen D, Mazumder S, Melo JS, Khan A, Bhattyacharya S, D'Souza SF. Evaporation driven self-assembly of a colloidal dispersion during spray drying: volume fraction dependent morphological transition. *Langmuir* 2009;**25**:6690–5.
31. Cheong YS, Adams MJ, Routh AF, Hounslow MJ, Salman AD. The production of binderless granules and their mechanical characteristics. *Chem Eng Sci* 2005;**60**:4045–53.
32. Omrane A, Santesson S, Alden M, Nilsson S. Laser techniques in acoustically levitated micro droplets. *Lab on a chip—miniaturisation for chemistry and biology* 2004;**4**(4):287–91.
33. EN 1991-4:2006. *Eurocode 1—actions on structures. Part 4: silos and tanks*.